Magnetic anisotropy in hole-doped superconducting Ba_{0.67}K_{0.33}Fe_{2}As_{2} probed by polarized inelastic neutron scattering

Chenglin Zhang, Mengshu Liu, Yixi Su, Louis-Pierre Regnault, Meng Wang, Guotai Tan, Th. Brückel, Takeshi Egami, and Pengcheng Dai

Phys. Rev. B **87**, 081101 — Published 7 February 2013

DOI: 10.1103/PhysRevB.87.081101

Magnetic anisotropy in hole-doped superconducting $Ba_{0.67}K_{0.33}Fe_2As_2$ probed by polarized inelastic neutron scattering

Chenglin Zhang,[1] Mengshu Liu,[1] Yixi Su,[2] Louis-Pierre Regnault,[3] Meng Wang,[1,4] Guotai Tan,[1,5] Th. Brückel,[6] Takeshi Egami,[1,7,8] and Pengcheng Dai[1,4,*]

[1]*Department of Physics and Astronomy, The University of Tennessee, Knoxville, Tennessee 37996-1200, USA*
[2] *Jülich Centre for Neutron Science JCNS-FRM II, Forschungszentrum Jülich GmbH, Outstation at FRM II, Lichtenbergstrasse 1, D-85747 Garching, Germany*
[3]*Institut Laue-Langevin, 6, rue Jules Horowitz, BP 156, 38042 Grenoble Cedex 9, France*
[4]*Beijing National Laboratory for Condensed Matter Physics, Institute of Physics, Chinese Academy of Sciences, Beijing 100190, China*
[5]*Physics Department, Beijing Normal University, Beijing 100875, China*
[6]*Jülich Centre for Neutron Science JCNS and Peter Grünberg Institut PGI, JARA-FIT, Forschungszentrum Jülich GmbH, 52425 Jülich, Germany*
[7]*Department of Materials Science and Engineering, The University of Tennessee, Knoxville, Tennessee 37996-1200, USA*
[8]*Joint Institute of Neutron Sciences, Oak Ridge National Laboratory, Oak Ridge, Tennessee 37831, USA*

(Dated: January 30, 2013)

We use polarized inelastic neutron scattering (INS) to study spin excitations of optimally hole-doped superconductor $Ba_{0.67}K_{0.33}Fe_2As_2$ ($T_c = 38$ K). In the normal state, the imaginary part of the dynamic susceptibility, $\chi''(Q,\omega)$, shows magnetic anisotropy for energies below ∼7 meV with c-axis polarized spin excitations larger than that of the in-plane component. Upon entering into the superconducting state, previous unpolarized INS experiments have shown that spin gaps at ∼5 and 0.75 meV open at wave vectors $Q = (0.5, 0.5, 0)$ and $(0.5, 0.5, 1)$, respectively, with a broad neutron spin resonance at $E_r = 15$ meV. Our neutron polarization analysis reveals that the large difference in spin gaps is purely due to different spin gaps in the c-axis and in-plane polarized spin excitations, resulting resonance with different energy widths for the c-axis and in-plane spin excitations. The observation of spin anisotropy in both opitmally electron and hole-doped $BaFe_2As_2$ is due to their proximity to the AF ordered $BaFe_2As_2$ where spin anisotropy exists below T_N.

PACS numbers: 74.70.Xa, 75.30.Gw, 78.70.Nx

Neutron polarization analysis has played an important role in determining the magnetic structure and excitations of solids[1]. For high-transition temperature (High-T_c) copper oxide superconductors derived from hole or electron-doping from their antiferromagnetic (AF) parent compounds, neutron polarization analysis have conclusively shown that the collective magnetic excitation coupled to superconductivity at the AF wave vector of the parent compounds, termed neutron spin resonance[2], has a magnetic origin[3–9]. Furthermore, by carrying out neutron polarization analysis with a spin-polarized incident neutron beam along the scattering wave vector $\mathbf{Q} = \mathbf{k}_i - \mathbf{k}_f$ (where $\mathbf{k}_i$ and $\mathbf{k}_f$ are the incident and final wave vectors of the neutron, respectively), $\hat{\mathbf{x}}||\mathbf{Q}$; perpendicular to $\mathbf{Q}$ but in the scattering plane, $\hat{\mathbf{y}}\perp\mathbf{Q}$; and perpendicular to $\mathbf{Q}$ and the scattering plane, $\hat{\mathbf{z}}\perp\mathbf{Q}$, one can use neutron spin flip (SF) scattering cross sections $\sigma^{\rm SF}_{xx}, \sigma^{\rm SF}_{yy}$, and $\sigma^{\rm SF}_{zz}$ to determine the spatial anisotropy of spin excitations[1]. If the resonance is an isotropic triplet excitation of the singlet superconducting ground state, one expects that the degenerate triplet would be isotropic in space as pure paramagnetic scattering[9]. For optimally hole-doped copper oxide superconductor $YBa_2Cu_3O_{6.9}$ ($T_c = 93$ K), neutron polarization analysis reveals that spin excitations in the normal state are spatially isotropic and featureless for energies $10 \le E \le 60$ meV, consistent with pure paramagnetic scattering. Upon entering into the superconducting state, a quasi-isotropic spin resonance occurs at $E_r = 40$ meV to within the precision of the measurements and a spin anisotropy develops in the lower energy $10 \le E \le 30$ meV, resulting in a clear spin gap below 22 meV for the c-axis polarized dynamic susceptibility χ''_c and in-plane $\chi''_{a/b}$ for $E \ge 10$ meV[6]. The low-energy spin anisotropy is likely due to spin-orbit coupling in the system. For optimally electron-doped copper oxide superconductor $Pr_{0.88}LaCe_{0.12}CuO_{4-\delta}$, spin excitations are isotropic both above and below T_c[8]. Therefore, the spin anisotropy in the superconducting state of hole-doped $YBa_2Cu_3O_{6.9}$ is unrelated to the normal state paramagnetic scattering.

Like copper oxide superconductors, superconductivity in iron pnictides also arises when electrons or holes are doped into their AF parent compounds[10–14]. Furthermore, unpolarized neutron scattering experiments have shown that both hole and electron-doped iron pnictides exhibits a neutron spin resonance similar to copper oxide superconductors[15–20]. In the initial polarized neutron scattering experiment on optimally electron-doped superconductor $BaFe_{1.9}Ni_{0.1}As_2$ ($T_c = 20$ K), χ''_c was found to be much larger than $\chi''_{a/b}$ for energies $2 \le E \le 6$ meV below T_c , while the resonance at $E_r = 7$ meV

is only weakly anisotropic[21]. In a subsequent polarized neutron scattering measurement on undoped AF parent compound $BaFe_2As_2$[22], isotropic paramagnetic scattering at low-energy ($E = 10$ meV) were found to become anisotropic spin waves below the Néel temperature T_N with a much larger in-plane ($\chi''_{a/b}$) spin gap than that of the out-of-plane gap (χ''_c). These results indicate a strong single-ion anisotropy and spin-orbit coupling, suggesting that more energy is needed to rotate a spin within the orthorhombic a-b plane than rotating it to the c-axis[22]. However, similar polarized neutron experiments on electron-overdoped $BaFe_{1.85}Ni_{0.15}As_2$ ($T_c = 14$ K), which is far away from the AF ordered phase, reveal isotropic paramagnetic scattering both above and below T_c[23]. Very recently, Steffens *et al.* report evidence for two resonance-like excitations in the superconducting state of optimally electron-doped $BaFe_{1.88}Co_{0.12}As_2$ ($T_c = 24$ K). In addition to an isotropic resonance at $E = 8$ meV with weak dispersion along the c-axis, there is a resonance at $E = 4$ meV polarized only along the c-axis with strong intensity variation along the c-axis[24]. In the normal state, there are isotropic paramagnetic scattering at AF wave vectors with $L = 0$ and weak anisotropic scattering with a larger c-axis polarized intensity at $L = 1$[24].

If the observed anisotropic magnetic scattering in the superconducting state of optimally electron-doped $BaFe_{1.9}Ni_{0.1}As_2$[21] and $BaFe_{1.88}Co_{0.12}As_2$[24] are indeed associated with the anisotropic spin waves in $BaFe_2As_2$[22], one would expect similar anisotropic spin excitations in hole-doped materials not too far away from the parent compound. In this paper, we report neutron polarization analysis on spin excitations of the optimally hole-doped superconducting $Ba_{0.67}K_{0.33}Fe_2As_2$. From the previous unpolarized INS work on the same sample, we know that spin excitations in the superconducting state have a resonance at $E_r = 15$ meV, a small spin gap ($E_g \approx 0.75$ meV) at $\mathbf{Q} = (0.5, 0.5, 0)$ and a large gap ($E_g = 5$ meV) at $(0.5, 0.5, 1)$[16]. In the normal state, spin excitations at both wave vectors are gapless and increase linearly with increasing energy[16]. Our polarized INS experiments reveal that the persistent low-energy spin excitations at the AF wave vector $(0.5, 0.5, 1)$ below T_c are entirely c-axis polarized. Although there is also superconductivity-induced spin anisotropy similar to optimally electron-doped $BaFe_{1.9}Ni_{0.1}As_2$[21] and $BaFe_{1.88}Co_{0.12}As_2$[24], the low-energy c-axis polarized spin excitations do not change across T_c and therefore cannot have the same microscopic origin as the spin isotropic resonance at $E_r = 15$ meV. We suggest that the persistent c-axis polarized spin excitations in the superconducting state of optimally hole and electron-doped iron pnictide superconductors is due to their proximity to the AF ordered parent compound. Their coupling to superconductivity may arise from different contributions of Fe $3d_{X^2-Y^2}$ and $3d_{XZ/YZ}$ orbitals to superconductivity[25].

Single crystals of $Ba_{0.67}K_{0.33}Fe_2As_2$ are grown by a self-flux method[16]. About 10 grams of single crystals are coaligned in the $[H, H, L]$ scattering plane (with mosaicity 3° at full width half maximum) with a tetragonal unit cell for which $a = b = 3.93$ Å, and $c = 13.29$ Å. In this notation, the vector $\mathbf{Q}$ in three-dimensional reciprocal space in Å^{-1} is defined as $\mathbf{Q} = H\mathbf{a}^* + K\mathbf{b}^* + L\mathbf{c}^*$, where H, K, and L are Miller indices and $\mathbf{a}^* = \hat{\mathbf{a}}2\pi/a, \mathbf{b}^* = \hat{\mathbf{b}}2\pi/b, \mathbf{c}^* = \hat{\mathbf{c}}2\pi/c$ are reciprocal lattice vectors. Our polarized INS experiments were carried out on the IN22 triple-axis spectrometer with Cryopad capability at the Institut Laue-Langevin in Grenoble, France. The fixed final neutron wave vectors were set at $k_f = 2.66$ Å^{-1} and $k_f = 3.84$ Å^{-1} in order to close the scattering triangles. To compare with previous polarized INS results on iron pnictides[21–24], we converted the measured neutron SF scattering cross sections $\sigma^{\rm SF}_{xx}$, $\sigma^{\rm SF}_{yy}$, and $\sigma^{\rm SF}_{zz}$ into c-axis (M_{001}) and in-plane (M_{110}) components of the magnetic

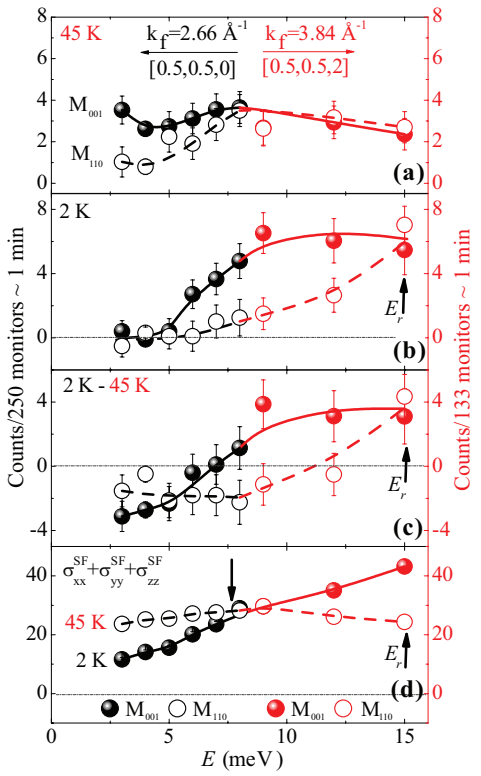

FIG. 1: (Color online) Neutron polarization analysis determined c-axis ($\chi''_c \propto M_{001}$) and in-plane ($\chi''_{a/b} \propto M_{110}$) components of spin excitations in $Ba_{0.67}K_{0.33}Fe_2As_2$ from raw SF constant-Q scans at $\mathbf{Q} = (0.5, 0.5, 0)$ and and $(0.5, 0.5, 2)$. To extract M_{001} and M_{110}, we use methods described in Ref.[23] and assume $M_{1\bar{1}0} = M_{110}$ in the tetragonal crystal. (a) Energy dependence of M_{001} and M_{110} at $T = 45$ K. (b) Identical scans at $T = 2$ K. (c) The solid and open circles show the temperature difference (2 K−45 K) for M_{001} and M_{110}, respectively. (d) The sum of $\sigma^{\rm SF}_{xx} + \sigma^{\rm SF}_{yy} + \sigma^{\rm SF}_{zz}$ at 45 and 2 K. Since background scattering is not expected to change between these temperatures[16], such a procedure will increase statistics of magnetic scattering. The black data points are collected at $\mathbf{Q} = (0.5, 0.5, 0)$ with $k_f = 2.66$ Å^{-1}, while the red data points are at $\mathbf{Q} = (0.5, 0.5, 1)$ with $k_f = 3.84$ Å^{-1}. The solid and dashed lines are guided to the eyes.

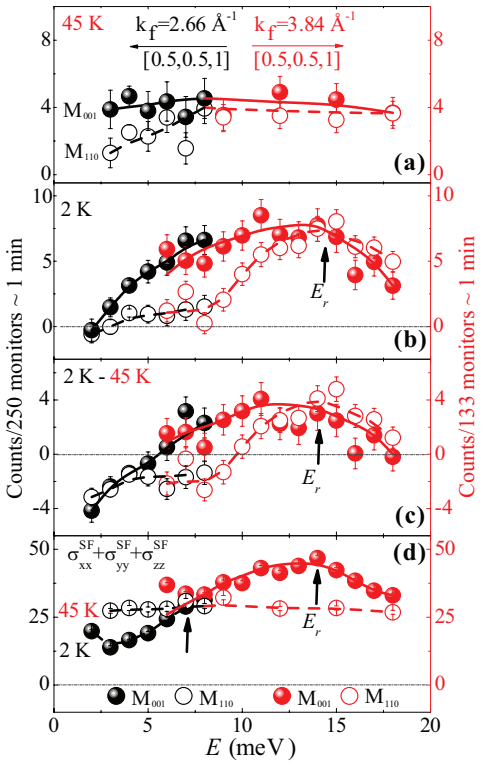

FIG. 2: (Color online) Constant-Q scans at $\mathbf{Q} = (0.5, 0.5, 1)$ below and above T_c. (a) Energy dependence of M_{001} and M_{110} at $T = 45$ K and (b) at 2 K. The superconductivity-induced spin gaps are at ≤ 2 and 7 meV for M_{001} and M_{110}, respectively. At resonance energy of $E_r = 15$ meV, the scattering is isotropic. (c) The solid and open circles show the temperature difference (2 K−45 K) for M_{001} and M_{110}, respectively. (d) The sum of $\sigma^{\rm SF}_{xx} + \sigma^{\rm SF}_{yy} + \sigma^{\rm SF}_{zz}$ at 45 and 2 K. The solid and dashed lines are guided to the eyes.

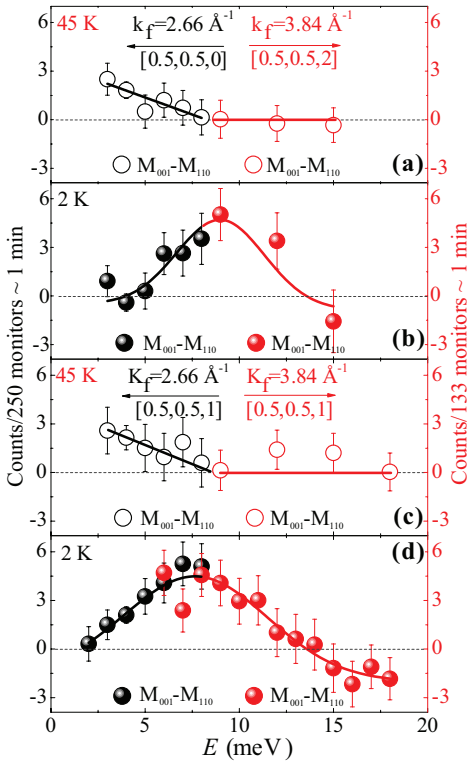

FIG. 3: (Color online) Energy dependence of spin anisotropy as determined by the difference between $M_{001} - M_{110}$ for temperatures (a) 45 K and (b) 2 K at wave vector $\mathbf{Q} = (0.5, 0.5, 0)$ and $\mathbf{Q} = (0.5, 0.5, 2)$. Similar differences above (c) and below (d) T_c at $\mathbf{Q} = (0.5, 0.5, 1)$. The energy width is broader in (d) compared with (b). The solid and dashed lines are guided to the eyes.

scattering[23].

Figure 1 shows energy scans above and below T_c at wave vectors $\mathbf{Q} = (0.5, 0.5, 0)$ and $(0.5, 0.5, 2)$. We chose these two equivalent wave vectors with different fixed final neutron energies to satisfy the kinematic condition for the large covered energy range. Since the iron magnetic form factors, geometrical factors, and instrumental resolutions are different at these two wave vectors, we use left and right scales for $\mathbf{Q} = (0.5, 0.5, 0)$ and $(0.5, 0.5, 2)$, respectively. In the normal state (45 K), spin anisotropy for energies below $E \approx 7$ meV is clear with M_{001} (χ''_c) larger than M_{110} ($\chi''_{a/b}$) [Fig. 1(a)]. For $E > 7$ meV, spin excitations are nearly isotropic. This is different from electron-doped $BaFe_{1.88}Co_{0.12}As_2$, where paramagnetic scattering at $\mathbf{Q} = (0.5, 0.5, 0)$ is isotropic above T_c[24]. In the superconducting state (2 K), M_{001} and M_{110} in $Ba_{0.67}K_{0.33}Fe_2As_2$ vanish below 5 meV, consistent with opening of a superconductivity-induced spin gap [Fig. 1(b)][16]. From $E = 5$ meV to the resonance energy at $E_r = 15$ meV, both M_{001} and M_{110} increase with increasing energy, but with different slope resulting significant spin anisotropy ($M_{001} > M_{110}$) appearing near $E \approx 8$ meV [Fig. 1(b)]. This is similar to the spin anisotropy in $BaFe_{1.88}Co_{0.12}As_2$[24]. Figure 1(c) shows the temperature difference of magnetic scattering, revealing net intensity gains for M_{001} and M_{110} only above ~7 and 10 meV, respectively. Figure 1(d) shows the sum of the SF magnetic scattering intensities for three different neutron polarizations, which improve the statistics, above and below T_c. Consistent with Fig. 1(c), the superconductivity-induced net magnetic intensity gain appears only above ~7 meV, forming a resonance at $E_r = 15$ meV.

Figure 2 summarizes the identical scans as that of Fig. 1 at the AF wave vector $\mathbf{Q} = (0.5, 0.5, 1)$ above and below T_c. At $T = 45$ K, we see clear spin anisotropy below $E \approx 7$ meV with $M_{001} > M_{110}$ similar to the spin excitations at $\mathbf{Q} = (0.5, 0.5, 0)$ [Fig. 2(a)]. Upon cooling to 2 K, a large spin gap opens below $E \approx 7$ meV in M_{110}, but there is still magnetic scattering in M_{001} extending to at least 2 meV. Therefore, the low-energy signal above ~1 meV at $\mathbf{Q} = (0.5, 0.5, 1)$ reported in the earlier unpolarized neutron measurements[16] are entirely c-axis polarized magnetic scattering. The neutron spin resonance at $E_r = 15$ is isotropic. The temperature difference plots

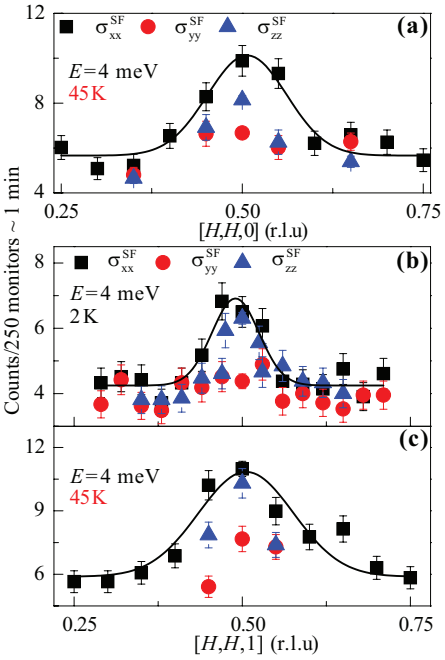

FIG. 4: (Color online) Constant-energy scans along the $[H,H,0]$ and $[H,H,1]$ directions at an energy transfer of $E = 4$ meV for different neutron polarization directions. (a) Neutron SF scattering cross sections $\sigma^{\rm SF}_{xx}$, $\sigma^{\rm SF}_{yy}$, and $\sigma^{\rm SF}_{zz}$ at 45 K along the $[H,H,0]$ direction. Similar scans along the $[H,H,1]$ direction at (b) 2 K and (c) 45 K. All data are obtained with $k_f = 2.66$ Å^{-1}. The solid lines are fit by Gaussian.

between 2 and 45 K display a broad and narrow peak for M_{001} and M_{110}, respectively [Fig. 2(c)]. Fig. 2(d) shows the sum of SF magnetic scattering below and above T_c. Consistent with unpolarized work[16], we see net intensity gain of the resonance in the superconducting state for energies above $E \approx 7$ meV, different from that of $BaFe_{1.88}Co_{0.12}As_2$ where the magnetic intensity starts to gain above $E = 4$ meV in the superconducting state [Fig. 4(b) in[24]].

To further illustrate the effect of spin anisotropy, we plot in Figs. 3(a)-3(d) the differences of $(M_{001} - M_{110})$ above and below T_c at wave vectors $\mathbf{Q} = (0.5, 0.5, 0)$ and $(0.5, 0.5, 1)$. In the normal state, we see clear magnetic anisotropy with $M_{001} > M_{110}$ for energies below ~7 meV [Figs. 3(a) and 3(c)]. In the superconducting state, the $(M_{001} - M_{110})$ differences reveal similar intensity peaks centered around ~7 meV at $\mathbf{Q} = (0.5, 0.5, 0)$ and $(0.5, 0.5, 1)$, but with a much broader width for $\mathbf{Q} = (0.5, 0.5, 1)$ [Figs. 3(b) and 3(d)]. Since there are essentially no intensity gain in M_{001} across T_c near ~7 meV [Figs. 1(c) and 2(c)], the apparent peaks in $(M_{001} - M_{110})$ arise from different responses of M_{001} and M_{110} across T_c. While the intensity of M_{001} across T_c is suppressed below ~7 meV and enhanced above it, similar cross over energy occurs around 10 meV in M_{110}, thus resulting peaks near 7 meV in $(M_{001} - M_{110})$ at 2 K [Figs. 3(b) and 3(d)]. Therefore, the differences in superconductivity-induced spin gaps in M_{001} and M_{110} at $\mathbf{Q} = (0.5, 0.5, 0)$ and $(0.5, 0.5, 1)$ are causing peaks in $(M_{001} - M_{110})$.

Finally, to confirm the low-energy spin anisotropy discussed in Figs. 1-3, we show in Figs. 4(a)-4(c) constant-energy scans with three different neutron polarizations at $E = 4$ meV along the $[H,H,0]$ and $[H,H,1]$ directions. In the normal state, $\sigma^{\rm SF}_{xx}$ shows clear peaks at $\mathbf{Q} = (0.5, 0.5, 0)$ and $(0.5, 0.5, 1)$ [Figs. 4(a) and 4(c)]. In both cases, we also find $\sigma^{\rm SF}_{xx} \geq \sigma^{\rm SF}_{zz} > \sigma^{\rm SF}_{yy}$, thus confirming the anisotropic nature of the magnetic scattering with $M_{001} > M_{110}$. In the superconducting state, while $\sigma^{\rm SF}_{xx}$ and $\sigma^{\rm SF}_{zz}$ are peaked at $(0.5, 0.5, 1)$, $\sigma^{\rm SF}_{yy}$ is featureless. These results again confirm the presence of a larger superconductivity-induced spin gap in M_{110} than that in M_{001} [Fig. 2(b)].

From Figs. 1-4, we see anisotropic spin susceptibility in both the normal and superconducting state of $Ba_{0.67}K_{0.33}Fe_2As_2$, different from optimally electron-doped $BaFe_{1.88}Co_{0.12}As_2$ where the anisotropy is believed to emerge only with the opening of the superconducting gap[24]. Furthermore, our data reveal that large differences in the superconductivity-induced spin gaps at $\mathbf{Q} = (0.5, 0.5, 0)$ and $(0.5, 0.5, 1)$[16] arise from the differences in spin gaps of c-axis polarized spin excitations. These results are similar to the previous work on electron-doped $BaFe_{1.9}Ni_{0.1}As_2$[21] and $BaFe_{1.88}Co_{0.12}As_2$[24], suggesting that the influence of a strong spin anisotropy in undoped parent compound $BaFe_2As_2$[22] extends to both optimally electron and hole-doped iron pnictide superconductors. For comparison, we note that spin excitations in superconducting iron chalcogenides are different, having slightly anisotropic resonance with isotropic spin excitations below the resonance[26,27].

In Ref.[24], it was suggested that the observed spin anisotropy in $BaFe_{1.88}Co_{0.12}As_2$ can be understood as a c-axis polarized resonance whose intensity strongly varies with the c-axis wave vector. This is not the case in $Ba_{0.67}K_{0.33}Fe_2As_2$ since we find much weaker c-axis modulation of the magnetic intensity[16]. Therefore, the spin anisotropy seen in optimally electron and hole-doped superconductors is a consequence of these materials being close to the AF ordered parent compound $BaFe_2As_2$, where spin-orbit coupling is expected to be strong[28–30], and is not fundamental to superconductivity of these materials. To understand how spin anisotropy in optimally hole and electron-doped iron pnictide superconductors might be coupled to superconductivity via spin-orbit interaction, we note that hole and electron-doped iron pnictides are multiband superconductors with different superconducting gaps for different orbitals. If c-axis and in-plane spin excitations arise from quasiparticle excitations of different orbitals between hole and electron Fermi pockets[31], the large differences in superconducting gaps for Fermi surfaces of different orbital characters might induce the observed large spin anisotropy.

We are grateful to W. C. Lv for helpful discussions and H.F. Li, K. Schmalzl, and W. Schmidt for their assistance in the neutron scattering experiment. The work

at UTK is supported by the US DOE BES No. DE-FG02-05ER46202. C.L.Z and T.E are partially supported by the US DOE BES through the EPSCoR grant, DE-FG02-08ER46528. Work at IOP is supported by the MOST of China 973 programs (2012CB821400).

* Electronic address: pdai@utk.edu

[1] R. M. Moon, T. Riste, and W. C. Koehler, Phys. Rev. **181**, 920 (1969).

[2] J. Rossat-Mignod, L. P. Regnault, C. Vettier, P. Bourges, P. Burlet, J. Bossy, J. Y. Henry and G. Lapertot, Physica C (Amsterdam) **185**, 86 (1991).

[3] H. A. Mook, G. Aeppli and T. E. Mason and T. Armstrong, Phys. Rev. Lett. **70**, 3490 (1993).

[4] H. F. Fong, B. Keimer, D. Reznik, D. L. Milius and I. A. Aksay, Phys. Rev. B **54**, 6708 (1996).

[5] Pengcheng Dai, H. A. Mook, R. D. Hunt and F. Doğan, Phys. Rev. B **63**, 054525 (2001).

[6] N. S. Headings, S. M. Hayden, J. Kulda, N. Hari Babu, and D. A. Cardwell. Phys. Rev. B **84**, 104513 (2011).

[7] S. D. Wilson, P. Dai, S. Li, S. Chi, H. J. Kang and J. W. Lynn, Nature (London) **442**, 59 (2006).

[8] J. Zhao, F. C. Niestemski, Shankar Kunwar, Shiliang Li, P. Steffens, A. Hiess, H. J. Kang, S. D.Wilson, Ziqiang Wang, P. C. Dai, and V. Madhavan, Nat. Phys. **7**, 719 (2011).

[9] M. Eschrig, Adv. Phys. **55**, 47 (2006).

[10] Y. Kamihara, T. Watanabe, M. Hirano, and H. Hosono, J. Am. Chem. Soc. **130**, 3296 (2008).

[11] M. Rotter, M. Tegel, and D. Johrendt, Phys. Rev. Lett. **101**, 107006 (2008).

[12] L. J. Li, Y. K. Luo, Q. B. Wang, H. Chen, Z. Ren, Q. Tao, Y. K. Li, X. Lin, M. He, Z. W. Zhu, G. H. Cao, and Z. A. Xu, New J. Phys. **11**, 025008 (2009).

[13] C. de la Cruz, Q. Huang, J. W. Lynn, J. Li, W. Ratcliff II, J. L. Zarestky, H. A. Mook, G. F. Chen, J. L. Luo, N. L. Wang, and P. Dai, Nature (London) **453**, 899 (2008).

[14] P. Dai, J. P. Hu, and E. Dagotto, Nat. Phys. **8**, 709 (2012).

[15] A. D. Christianson, E. A. Goremychkin, R. Osborn, S. Rosenkranz, M. D. Lumsden, C. D. Malliakas, I. S. Todorov, H. Claus, D. Y. Chung, M. G. Kanatzidis, R. I. Bewley, and T. Guidi, Nature (London) **456**, 930 (2008).

[16] C. L. Zhang, M. Wang, H. Q. Luo, M. Y. Wang, M. S. Liu, J. Zhao, D. L. Abernathy, T. A. Maier, K. Marty, M. D. Lumsden, S. Chi, S. Chang, J. A. Rodriguez-Rivera, J. W. Lynn, T. Xiang, J. P. Hu, and Pengcheng Dai, Scientific Report **1**, 115 (2011).

[17] M. D. Lumsden, A. D. Christianson, D. Parshall, M. B. Stone, S. E. Nagler, G. J. MacDougall, H. A. Mook, K. Lokshin, T. Egami, D. L. Abernathy, E. A. Goremychkin, R. Osborn, M. A. McGuire, A. S. Sefat, R. Jin, B. C. Sales and D. Mandrus, Phys. Rev. Lett. **102**, 107005 (2009).

[18] S. Chi, A. Schneidewind, J. Zhao, L. W. Harriger, L. Li, Y. Luo, G. Cao, Z. Xu, M. Loewenhaupt, J. Hu and P. Dai, Phys. Rev. Lett. **102**, 107006 (2009).

[19] D. S. Inosov, J. T. Park, P. Bourges, D. L. Sun, Y. Sidis, A. Schneidewind, K. Hradil, D. Haug, C.T. Lin, B. Keimer and V. Hinkov, Nat. Phys. **6**, 178 (2010).

[20] H. Q. Luo, Z. Yamani, Y. C. Chen, X. Y. Lu, M. Wang, S. L. Li, T. A. Maier, S. Danilkin, D. T. Adroja, and P. Dai, Phys. Rev. B **86**, 024508 (2012).

[21] O. J. Lipscombe, L. W. Harriger, P. G. Freeman, M. Enderle, C. L. Zhang, M. Y. Wang, T. Egami, J. P. Hu, T. Xiang, M. R. Norman, and Pengcheng Dai, Phys. Rev. B **82**, 064515 (2010).

[22] N. Qureshi, P. Steffens, S. Wurmehl, S. Aswartham, B. Büchner, and M. Braden, Phys. Rev. B **86**, 060410 (2012).

[23] M. S. Liu, C. Lester, J. Kulda, X. Y. Lu, H. Q. Luo, M. Wang, S. M. Hayden, and Pengcheng Dai Phys. Rev. B **85**, 214516 (2012).

[24] P. Steffens, C. H. Lee, N. Qureshi, K. Kihou, A. Ayo, H. Eisaki, and M. Braden, arXiv:1210.6386.

[25] W. Malaeb *et al.*, Phys. Rev. B **86**, 165117 (2012).

[26] P. Babkevich, B. Roessli, S. N. Gvasaliya, L.-P. Regnault, P. G. Freeman, E. Pomjakushina, K. Conder, and A. T. Boothroyd, Phys. Rev. B **83**, 180506(R) (2011).

[27] K. Prokeš, A. Hiess, W. Bao, E. Wheeler, S. Landsgesell, and D. N. Argyriou, Phys. Rev. B **86**, 064503 (2012).

[28] F. Krüger, S. Kumar, J. Zaanen, and J. van den Brink, Phys. Rev. B **79**, 054504 (2009).

[29] C. C. Lee, W. G. Yin, and W. Ku, Phys. Rev. Lett. **103**, 267001 (2009).

[30] W. C. Lv and P. Phillips, Phys. Rev. B **84**, 174512 (2012).

[31] J. H. Zhang, R. Sknepnek, and J. Schmalian, Phys. Rev. B **82**, 134527 (2010).